Amide Hydrogen Exchange Determined by Mass Spectrometry: Application to Rabbit Muscle Aldolase[†]

Zhongqi Zhang,[‡,§] Carol Beth Post,[||] and David. L. Smith*,[‡]

Department of Chemistry, University of Nebraska−Lincoln, Lincoln, Nebraska 68588-0304, and Department of Medicinal Chemistry, Purdue University, West Lafayette, Indiana 47907

Received September 18, 1995; Revised Manuscript Received November 14, 1995[⊗]

ABSTRACT: The protein fragmentation/mass spectrometry method described by Zhang and Smith [(1993) *Protein Sci. 2*, 522−531] has been extended to measure amide hydrogen exchange rates in rabbit muscle aldolase, a homotetramer with $M_r = 157\,000$. Following a period of deuterium exchange, the partially deuterated protein was proteolytically fragmented into peptides whose deuterium contents were determined by directly coupled HPLC fast atom bombardment mass spectrometry. Hydrogen exchange rates were determined for amide hydrogens located in short segments derived from 85% of the aldolase backbone. Isotopic exchange rate constants spanning the range from 100 to 0.001 h^{-1} were determined for the exchange-in times used in this study (2.5 min to 44 h). The exchange rates for amide hydrogens located within short segments differed by as much as 10^4, demonstrating that local structural features dramatically affect the isotopic exchange rates in large proteins. A high level of correlation between the slowing of hydrogen exchange and intramolecular hydrogen bonding in aldolase was found. An exception to this correlation occurs at the subunit interface, where the amide hydrogens in one peptide segment with few amide hydrogen bonds have slower exchange rates than expected, suggesting that the amide hydrogens in this region are effectively shielded from the deuterated solvent. Isotope patterns observed for most peptides were binomial, indicating that hydrogen exchange proceeds through the EX2 mechanism (uncorrelated exchange). However, bimodal isotope patterns were found for peptides derived from three short segments of aldolase (including residues 58−64, 279−283, and 326−337), suggesting structural differences in these regions. A high level of correlation was found between crystallographic *B*-factors and amide hydrogen exchange rates, suggesting an isotopic exchange mechanism involving localized low-amplitude, high-frequency motions that do not require collective motion of many residues. From a methodology viewpoint, these results demonstrate that the combination of protein fragmentation with mass spectrometry is a useful method for determining the rates at which amide hydrogens located over major portions of large proteins undergo isotopic exchange.

Isotopic exchange rates of amide hydrogens have long been used to provide information about the high-order structure, structural changes, and structural dynamics of proteins. At pH 7, the half-lives for isotopic exchange of peptide amide hydrogens in a protein may be as short as seconds or as long as months. Although the details of the mechanism of hydrogen exchange in proteins are not fully understood, the rates at which amide hydrogens in proteins undergo isotopic exchange appear to depend on whether the hydrogens are participating in intramolecular hydrogen bonding, as well as on the extent to which the hydrogens are shielded from the solvent. Therefore, amide hydrogen exchange rates are a sensitive probe of protein structure and conformational fluctuations (Woodward et al., 1982; Englander et al., 1984). This information has been used to better understand the functions of proteins whose average structures were determined by X-ray crystallography (Louie et al., 1988; Englander et al., 1992; Kim et al., 1993). Hydrogen exchange has also proved useful for studies of proteins for which the structures of two functionally different states are similar, while their stabilities and hydrogen exchange rates are substantially different (Kaminsky & Richards, 1992; Marmorino et al., 1993). Such differences in hydrogen exchange behavior suggest that hydrogen exchange may be an important source of information about the dynamic processes proteins undergo. Similarly, hydrogen exchange has been used to investigate the structure and dynamics of proteins in functionally different forms of protein that are not amenable to analysis by X-ray crystallography (Jeng et al., 1990; Hughson et al., 1990; Henry & Sykes, 1990; Muga et al., 1991). Hydrogen exchange has also proved useful for identifying intermediates formed during protein folding and unfolding (Roder et al., 1988; Loftus et al., 1986; Baldwin, 1993; Englander & Mayne, 1992; Miranker et al., 1993; Jones & Matthews, 1995; Bai et al., 1995) and in studies of protein−protein complexation (Brandt & Woodward, 1987; Paterson et al., 1990; Mayne et al., 1992; Benjamin et al., 1992; Loh et al., 1993).

Experimental methods used to determine isotopic exchange rates of amide hydrogens without regard for their locations in proteins include infrared spectroscopy (Hvidt & Nielsen, 1966; Muga et al., 1991; de Jong et al., 1995), ultraviolet

[†] This work was supported through a grant (RO1 GM4038) to D.L.S. from the National Institutes of Health.

* Author to whom correspondence should be addressed; telephone, (402) 472-2794; fax, (402) 472-9862; e-mail, dls@unlinfo.unl.edu.

[‡] University of Nebraska.

[§] Present address: National High Magnetic Field Laboratory, 1800 E. Paul Dirac Dr., Tallahassee, FL, 32306-4005.

[||] Purdue University.

[⊗] Abstract published in *Advance ACS Abstracts,* January 1, 1996.

0006-2960/96/0435-779$12.00/0

spectroscopy (Englander et al., 1979; Loftus et al., 1986), and electrospray ionization mass spectrometry (Katta & Chait, 1991, 1993; Miranker et al., 1993; Wagner & Anderegg, 1994). Although much useful information has been obtained through numerous applications of these methods, they give no information about specific regions undergoing structural or dynamic changes. To understand the protein structure−function relationship, we must know which regions within a protein are changing. Highly detailed information of this type has been obtained for small proteins by using NMR[1] to measure isotopic exchange rates of individual amide hydrogens [see, for example, Wagner and Wüthrich (1982); Delepierre et al., 1987; Tüchsen & Woodward, 1987; Jeng et al., 1990] and by neutron diffraction (Kossiakoff, 1982; Bentley et al., 1983). Although the exchange rates of individual amide hydrogens can be determined by NMR, hydrogen exchange studies using NMR are restricted to highly soluble proteins with M_r values of less than approximately 20 000. Moreover, many amide hydrogens are not included in hydrogen exchange studies because their resonances have not been assigned or because they exchange too quickly to be detected. As a result, the exchange rates of surface amide hydrogens often cannot be measured because they exchange before the analysis is completed (Marmorino et al., 1993).

A method for determining amide hydrogen exchange rates with intermediate spatial resolution that is potentially suitable for investigations of large proteins has been described by Rosa and Richards (1979), as well as by Englander et al. (1985). Following the incubation of a protein in tritiated water, isotopic exchange in specific segments of the protein is quantified by fragmenting the protein with an acid protease, isolating the peptides, and determining the levels of tritium per molecule of peptide. This approach, known as the protein fragmentation method, has been applied to relatively large proteins. However, to quantify the peptides and measure their tritium levels, each peptide must be purified to homogeneity on a time scale that is short relative to the half-life for hydrogen exchange. As a result, only a few peptides can usually be used as probes (Mallikarachchi et al., 1989; Englander et al., 1992). Recently, Zhang and Smith (1993) reported an extension of this method (protein fragmentation/MS) in which deuterium was substituted for tritium, and the deuterium contents of peptides were determined by directly coupled HPLC and fast atom bombardment mass spectrometry (FABMS). Because the amide deuterium level was determined directly from the molecular weights of the peptides, it was not necessary to isolate the peptides prior to analysis. By optimizing the chromatography for speed rather than resolution, the extent of back-exchange occurring during analysis was relatively small. Furthermore, experimental conditions were chosen to generate and detect peptides representative of major parts of the protein backbone. These and other features make the protein fragmentation/MS method potentially useful for obtaining spatially resolved hydrogen exchange information on large proteins. For example, Liu and Smith (1994) applied the method to bovine α-crystallin, a lens protein composed of two gene products with monomer molecular weights of 20 000 and an aggregate molecular weight approaching 1 million. Recently, Johnson and Walsh (1994) studied the differences between apo- and holomyloglobin by a variant of this method in which electrospray ionization mass spectrometry was used in place of FABMS.

The protein fragmentation/MS method has now been used to investigate amide hydrogen exchange in rabbit muscle aldolase (D-fructose-1,6-bisphosphate D-glyceraldehyde-3-phosphate-lyase). This ubiquitous glycolytic enzyme plays a central role in glycolysis and fructose metabolism by catalyzing the reversible aldol cleavage of fructose 1,6-bisphosphate (Fru-1,6-P2) into the triose phosphates, D-glyceraldehyde 3-phosphate and dihydroxyacetone phosphate. The crystal structure of rabbit muscle aldolase, determined to a resolution of 2.7 Å, indicates that it is a tetramer with four identical subunits spatially related by 222-fold symmetry (Sygusch et al., 1985, 1987; Sygusch & Beaudry 1985). The molecular weight of the aldolase tetramer is 157 000, making it much too large for hydrogen exchange studies by high-resolution NMR. The goal of this study was to investigate the structural and dynamic features of rabbit muscle aldolase through peptide amide hydrogen exchange determined by the protein fragmentation/MS method. Concepts developed through previous studies of hydrogen exchange in much smaller proteins are used to relate the present results to the secondary, tertiary, and quaternary structures of aldolase.

MATERIALS AND METHODS

Materials. Rabbit muscle aldolase, pepsin, carboxypeptidase Y, carboxypeptidase A, anhydrous monobasic potassium phosphate, anhydrous dibasic potassium phosphate, and monothioglycerol were purchased from Sigma Chemical Co. Glycerol was purchased from Mallinckrodt Chemical. Deuterium oxide (99.9 atom % D) and trifluoroacetic acid were purchased from Aldrich Chemical Co., and Sephadex G-10 was purchased from Pharmacia Biotech. All materials were used without further purification.

Identification of Peptides. In preparation for the hydrogen exchange experiments, peptides formed by peptic digestion of aldolase under the quenching conditions used in this study (5 min, pH 2.4, 0 °C) were identified by off-line HPLC and FABMS. Aldolase was dissolved in 5 mM phosphate buffer to a concentration of 0.25 mM (monomer concentration) and digested with pepsin (1:1 enzyme/substrate). The digest was fractionated by reversed-phase HPLC. Fractions were collected, dried, and analyzed by FABMS to determine the molecular weights of the peptides. The identities of the peptides were determined by computer-assisted analysis of the molecular weight information (Zhou & Smith, 1990; Zhang & Smith, 1993) and confirmed by C-terminal sequencing with carboxypeptidases (Caprioli & Fan 1986; Smith et al., 1992) or collision-induced dissociation experiments (Biemann, 1990).

Deuterium Exchange In. Prior to exposure to D_2O, aldolase (0.5 nmol/μL) was equilibrated in 5 mM phosphate/H_2O buffer (pH 5.7) for approximately 1 h. To initiate isotopic exchange, the protiated solvent was rapidly (<1 min) replaced with deuterated solvent (5 mM KH_2PO_4) by using a spinning Sephadex G-10 gel filtration column (3 mL bed volume) (Jeng et al., 1990). The pD of the exchange-in

[1] Abbreviations: NMR, nuclear magnetic resonance spectroscopy; MS, mass spectrometry; FABMS, fast atom bombardment mass spectrometry; HPLC, high-performance liquid chromatography; TFA, trifluoroacetic acid; NOE, nuclear Overhauser effect.

solution with aldolase was 6.53. Values given in the text for pH and pD were taken directly from the pH meter and were not corrected for isotopic effects (Englander et al., 1985). The protein/D_2O solution was incubated at 25 °C for various times (from 2.5 min to 44 h) to facilitate isotopic exchange. Twenty microliter aliquots of this solution were taken at different times and combined with 7 μL of quench solution (0.1 M phosphate buffer/D_2O, pD 2.2) to decrease the pD to 2.6, thereby quenching the isotopic exchange reaction. The samples were stored at −70 °C until analysis.

Quantification of Deuterium. To determine the extent of deuterium incorporation into aldolase during the incubation time, the samples were thawed rapidly, digested with pepsin, and analyzed by directly coupled HPLC FABMS. Adequate digestion of aldolase was achieved within 5 min by adding 5 μL of pepsin/D_2O, followed by the addition of 13 μL of quench solution to adjust the pD to 2.4 (1:1 enzyme/substrate). Digestion was carried out for 5 min at 0 °C.

The microbore HPLC system and the continuous-flow FABMS probe used to interface the HPLC to the mass spectrometer have been described previously (Zhang & Smith, 1993). The HPLC system consisted of two Rainin pumps, a Rheodyne 8125 injector fitted with a 50 μL loop, and a 0.1 × 10 cm reversed-phase column (Aquapore RP300, C-8, 7 μm). Peptides were eluted with a gradient (0−40% CH_3CN in 12 min) where both mobile phases contained trifluoroacetic acid, glycerol, and monothioglycerol (0.05%, 3%, and 3%, respectively). The flow rate through the column was 100 μL/min. The effluent from the column was split (33:1), reducing the flow to the mass spectrometer to 3 μL/min. A 10-port valve (Valco C10U) was used to divert salts eluted from the column away from the FAB probe. A third pump (Harvard Apparatus) was used to provide continuous solvent flow to the probe while the effluent from the column was diverted. All components of the HPLC system, from the injector to the continuous-flow FAB probe, were submerged in an ice−water bath to minimize deuterium back-exchange.

Mass spectrometric analyses were performed with a Kratos MS-50 FAB mass spectrometer, which was operated with a xenon gun and an accelerating potential of 8 kV. Two HPLC FABMS analyses were performed for each exchange-in time. In one analysis, the mass spectrometer scanned the mass range from 1430 to 420 at a rate of 10 s/decade of mass in the centroid data acquisition mode and at a resolution of 1500. In the other analysis, the mass spectrometer scanned from 2800 to 1400 at a rate of 30 s/decade in the continuum data acquisition mode and at a resolution of 1000. Mass spectra were recorded with a Kratos DS-90 data acquisition system and then transferred to a Sun workstation. The centroid data were analyzed with software written by the authors, and the raw data were analyzed with Kratos Mach 3 software. The deuterium contents of peptides could normally be determined to within 0.1.

RESULTS

Peptic Digestion of Aldolase. The principal procedural steps in the protein fragmentation/MS method are as follows: (1) isotopic exchange for a specified time; (2) quenching isotopic exchange by decreasing the pH to approximately 2.5 and lowering the temperature to 0 °C; (3) fragmenting the partially deuterated protein into peptides with an acid protease; and (4) determining the molecular weights of the partially deuterated peptides by directly coupled HPLC FABMS (Zhang & Smith, 1993). The half-life for amide hydrogen exchange under quenching conditions is approximately 1 h, allowing sufficient time for analysis prior to major losses of deuterium. Pepsin was used to fragment the protein because it is an aggressive acid protease capable of cleaving most proteins at many sites. A series of experiments using different digestion times and enzyme:substrate ratios was performed to find the conditions that gave the largest number of peptides in the shortest time. From these experiments, it was determined that approximately 100 different peptides could be detected for a 5 min digestion time and an enzyme:substrate ratio of 1:1. The amino acid sequence of rabbit muscle aldolase (Lai et al., 1974) is presented in Figure 1, with arrows indicating 64 peptides used in this study. From this group of peptides, it was possible to determine the peptide amide deuterium level in 85% of the entire aldolase backbone. Peptides derived from four regions (residues 133−143, 229−246, 270−278, and 362−363) were not detected. Failure to detect peptides from some regions may be because their mass-to-charge ratios were outside the range scanned, because FABMS does not respond well to these peptides, or because the peptides were not retained by the reversed-phase HPLC column.

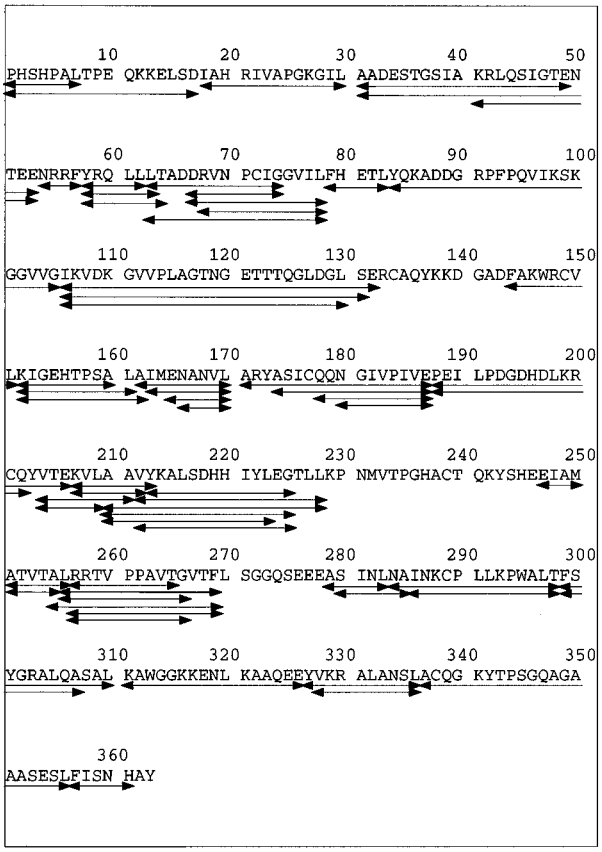

FIGURE 1: Amino acid sequence of rabbit muscle aldolase (Lai et al., 1974). Arrows indicate the peptides used in this study to determine the deuterium level along the backbone of the protein.

Peptide Analysis. Although digestion and HPLC fractionation were performed under quenching conditions and required less than 17 min, some artifactitious isotopic exchange of peptide amide hydrogen did occur. To minimize deuterium loss from the peptide amide linkages during HPLC fractionation, the extent of deuterium loss from a group of

13 completely deuterated peptides derived from aldolase was determined by using different levels of TFA (0.02−0.1%) in the mobile phase. The retention of peptide amide deuterium was different for each peptide as expected because of the inductive affects of the adjacent side chains (Molday et al., 1972; Bai et al., 1993). Furthermore, the TFA level leading to the maximum retention of deuterium was not the same for all peptides. However, the maximum retention averaged over the 13 peptides was 67% for a TFA concentration of 0.05%, which establishes the pH at 2.2.

During digestion, some deuterium exchanges into the protein from the D_2O solvent, even though the isotopic exchange rate is quenched at this temperature and pD. Likewise, some amide deuterium is replaced with hydrogen from the mobile phase (H_2O/CH_3CN) during HPLC fractionation. To compensate for this artifactitious isotopic exchange, two control samples of aldolase were analyzed by using standard conditions for digestion and HPLC fractionation (Zhang & Smith, 1993). A completely deuterated aldolase sample (100% control) was used to determine the amount of deuterium lost during analysis, while an unlabeled aldolase sample (0% control) was used to assess the quantity of deuterium gained during the analysis. Aldolase used for the 100% control was prepared by incubating aldolase in D_2O at 40 °C for 3 h at neutral pD, followed by incubation at pD 2.4 and 40 °C for another 3 h. The 0% control was prepared by dissolving aldolase directly into a solution equivalent to the postquench solution, followed by digestion and analysis by the normal procedure. The average molecular weights determined for peptides from the 100% control are equivalent to the molecular weights that would be detected when this segment is fully deuterated in the protein, while the average molecular weights determined for peptides from the 0% control are equivalent to the molecular weights that would be detected when this segment in the protein had no deuterium. The deuterium contents of partially deuterated peptides, adjusted for the gain and loss of deuterium during analysis, were obtained from the following expression:

$$D = \left(\frac{m - m_{0\%}}{m_{100\%} - m_{0\%}}\right)N \qquad (1)$$

where D is the deuterium content in a particular peptide and $m_{0\%}$, m, and $m_{100\%}$ are the average molecular weights of the same peptide in the zero-time control, partially deuterated sample, and fully deuterated control, respectively. The total number of peptide amide hydrogens in the peptide is given by N.

Application of eq 1 may be illustrated by using the FAB mass spectra presented in Figure 2 for the 284−298 segment of aldolase, which has 15 residues. Since this segment contains two Pro residues, it has a total of 12 peptide amide hydrogens (i.e., $N = 12$). The molecular weight of this segment, averaged over the natural distribution of isotopes (^{12}C, ^{13}C, etc.), is 1682.1 and would be recorded as MH^+ at *m/z* 1683.1. The FAB mass spectra of this peptide derived from the 0% control, aldolase incubated for $t = 3$ h, and 100% control are presented in Figure 2A−C. The average *m/z*'s for the MH^+ ions for the 284−298 segment from each of these samples, determined from the centroids of the peaks, are given. From these results, it is evident that this segment has 1.3, 5.5, and 9.8 mol atoms of deuterium in the 0% control, aldolase that was incubated in D_2O for 3 h, and 100% control, respectively. Application of eq 1 to these results shows that the deuterium content of this segment, adjusted for isotopic exchange during analysis, was 5.9. Although the locations of deuterium along the backbone of this segment cannot be determined from these data, all are believed to be located on peptide amide linkages because deuterium located on other functional groups (e.g., OD) is lost in the HPLC step (Englander et al., 1985).

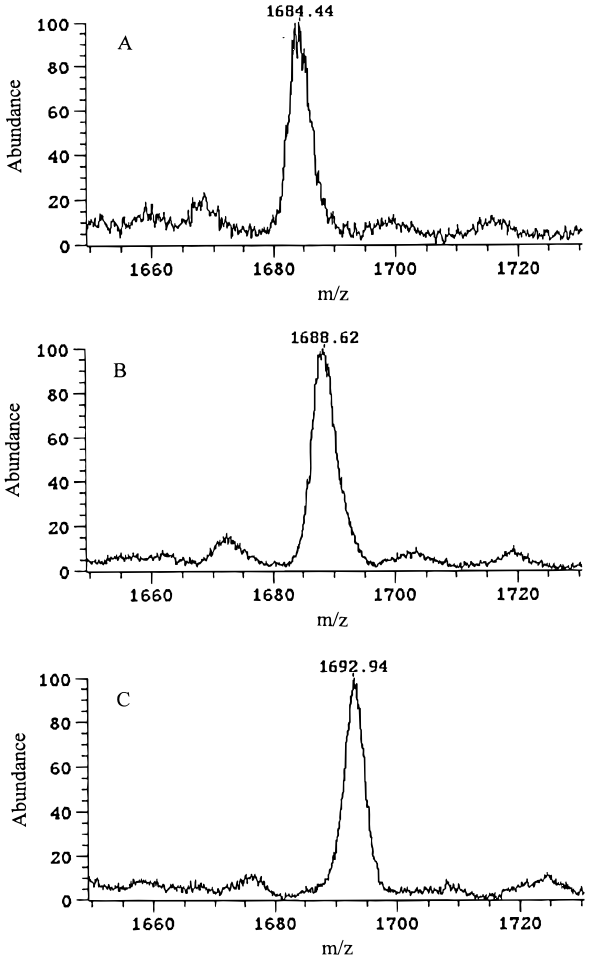

FIGURE 2: Mass spectra of the MH^+ ion of the peptide comprising residues 284−298 derived from (A) 0% control aldolase, (B) aldolase that had been incubated in D_2O for 3 h, and (C) 100% control aldolase.

Rates of Amide Isotopic Exchange. Deuterium levels in the 64 sensor peptides (see Figure 1) derived from aldolase that had been incubated in D_2O for various times were determined by the procedure described earlier. The extent of isotopic exchange within the segments represented by the sensor peptides can be visualized through plots of the level of deuterium per peptide molecule versus incubation time. For example, the deuterium level in the segment comprising peptide amides on residues 300−307 is determined from the peptide containing residues 299−307. Deuterium located on the primary amine of the amino terminus exchanges too rapidly under the quenching conditions to be detected. Deuterium exchange-in results for the 300−307 segment of aldolase, presented in Figure 3, indicate that seven of the eight peptide amide hydrogens in this segment are replaced with deuterium within approximately 2 h, while the last amide hydrogen resists exchange after incubation in D_2O for 44 h.

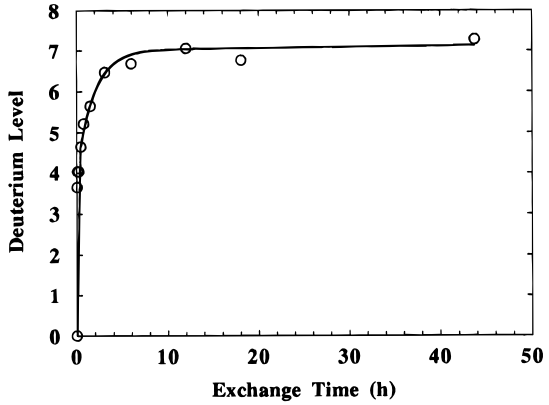

FIGURE 3: Number of deuteriums at peptide amide positions in segment 300−307, adjusted for isotopic exchange during analysis, presented as a function of the time aldolase was incubated in D_2O.

Conversion of time course data into rate data leads to a more quantitative interpretation of these results. When the deuterium concentration in the solution is large and the pH and temperature are constant, isotopic exchange of each amide hydrogen follows first-order kinetics (Englander & Kallenbach, 1984). Since each peptide contains several amide hydrogens, the deuterium content of a peptide can be described by the sum of N exponential terms:

$$D = n - \sum_{i=1}^{N} \exp(-k_i t) \qquad (2)$$

where D is the deuterium content of a peptide, k_i is the exchange rate constant for each amide hydrogen, and t is the time allowed for isotopic exchange. The exchange rate constants, k_i, were varied to obtain the best fit between eq 2 and the exchange-in data (Kaleidagraph, Abelbeck Software). This procedure led to the determination of the distribution of isotopic exchange rate constants of peptide amide hydrogens located within a segment. During the fitting process, some amide hydrogens have the same or very similar exchange rate constants and cannot be distinguished by the experimental data. Application of eq 2 to the data presented in Figure 3 indicates that, among the eight amide hydrogens in the 300−307 segment, four have exchange rate constants of approximately 53 h^{-1}, three have exchange rate constants of approximately 0.5 h^{-1}, and one has an exchange rate constant of less than 0.003 h^{-1}.

Although the range of rate constants for isotopic exchange can be determined by this procedure, the spatial resolution of the protein fragmentation method is limited primarily by the length of the sensor peptides. For the 64 peptides used in this study (see Figure 1), the average segment length is 13 peptide linkages, with the shortest and longest segments being 3 and 26 linkages, respectively. The spatial resolution can be enhanced in some regions of the protein by analyzing the difference in deuterium levels in overlapping peptides. In favorable cases, this procedure leads to determination of the isotopic exchange rate for a specific peptide linkage. This resolution enhancement procedure is illustrated for the segment comprising residues 308−310, where the deuterium level in this segment, as determined from the difference in the deuterium levels in segments 300−310 and 300−307, is plotted in Figure 4. Isotopic exchange rate constants obtained by fitting eq 2 to deuterium exchange-in data (Figures 3 and 4) for 58 segments of aldolase are given in Table 1 of the supporting information. For the conditions used in this study, the average segment contains five peptide linkages.

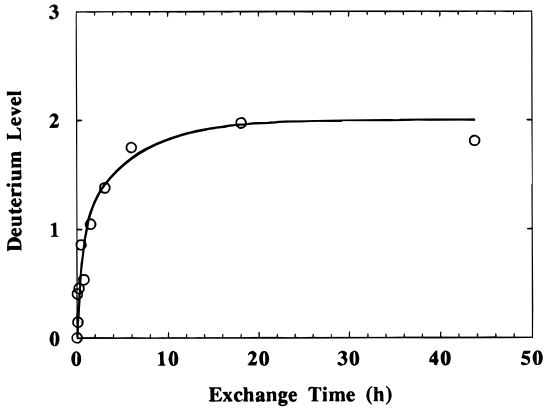

FIGURE 4: Number of deuteriums at peptide amide positions in segment 308−310 presented as a function of the time aldolase was incubated in D_2O. These results were derived from the difference in deuterium levels in segments 300−310 and 300−307.

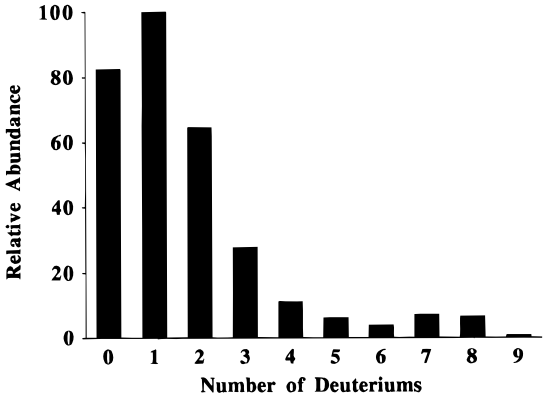

FIGURE 5: FABMS isotope pattern of peptide 327−336 derived from aldolase that had been incubated in D_2O for 6 h, illustrating a bimodal distribution of deuterium. This pattern has been adjusted for the natural abundance of heavy isotopes.

Deuterium Distribution Pattern. The distribution of deuterium atoms per molecule for the entire ensemble of sensor peptides is measured directly by mass spectrometry and may be an important source of information. When the determined isotope patterns of the peptides were adjusted for the natural abundance of heavy isotopes (e.g., ^{13}C, ^{15}N, etc.; Zhang & Smith, 1993), nearly all of the deuterium distribution patterns had the form of a single binomial distribution. This isotope pattern is expected when hydrogen exchange occurs randomly among the molecules in a sample. The rate of hydrogen exchange at different peptide linkages within molecules may be, and usually is, very different. The isotope patterns of several peptides, most notably those representing segments 58−62, 58−63, 58−64, 279−283, 326−336, 327−335, 327−336, 327−337, and 328−336, had the form of two binomial distributions. For example, the isotope pattern of the peptide composed of residues 327−336 is illustrated in Figure 5 after adjustment for the natural abundance of heavy isotopes. Isotope patterns for the same peptides derived from unlabeled aldolase, as well as for the 0% and 100% control samples, have the form of one binomial distribution, indicating that the observed bimodal distributions of isotopes are directly related to the hydrogen exchange process.

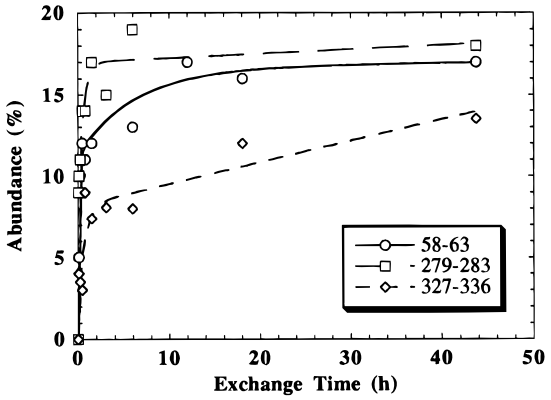

FIGURE 6: Plots of the relative amounts of the fast exchanging peptide units versus incubation time. Results were determined by analyzing bimodal isotope patterns of these peptides, as described in the Appendix.

The distribution of deuterium among the peptide molecules derived from a segment of the protein may be an important source of information regarding localized structural features of the protein or information about the kinetic mechanism through which isotopic exchange occurred. To extract such information from detected isotope patterns, we have developed a method to quantitatively describe the distribution of deuterium among the peptide amide linkages in the peptide molecules derived from a particular segment of a protein. This treatment considers that each segment with $N + 1$ amino acids has $N - P$ peptide amide hydrogens, where P is the number of linkages involving proline. Each of these peptide amide hydrogens has a specific rate constant for isotopic exchange; the range of these rate constants may be wide. Following a period of incubation in D_2O, the amide hydrogens at some linkages will be completely replaced with deuterium, while amide hydrogens at other linkages will have undergone little isotopic exchange. The centroids and widths of the detected isotopic distributions detected by mass spectrometry depend on the number of peptide linkages that have undergone complete, partial, or no isotopic exchange. This treatment, which is described in detail in the Appendix, was used to calculate bimodal isotope patterns, which were compared to the detected isotope patterns (Figure 5). When this analysis was applied to all of the detected bimodal deuterium isotope patterns (e.g., Figure 5), it was found that the group of peptides with the lower deuterium levels were only partially deuterated for all exchange times used in this study. Furthermore, the relative number of peptide molecules in this group decreased, and their average deuterium levels increased with increasing exchange time. In contrast, the group of peptide molecules with higher deuterium levels was completely deuterated for all exchange times. With increasing exchange time, only the relative number of peptide molecules in this group increased, as illustrated for three segments in Figure 6. Similar analyses of all peptides with bimodal isotope patterns showed that the relative abundances of this group of peptide molecules reached plateau values of 12−18%.

DISCUSSION

The structure and dynamics of proteins have been investigated via rates of peptide amide hydrogen exchange for 4 decades (Linderstrom-Lang, 1955; Hvidt & Nielsen, 1966). From these pioneering studies, it was learned that isotopic exchange rate constants for peptide amide hydrogens in folded proteins differ by many orders of magnitude. Half-lives for isotopic exchange, which depend on the structure and environment of the protein, typically span the range from seconds to months at pH 7. Models proposed to explain the wide range of exchange rates suggested that these rates likely are sensitive to protein dynamics (Linderstrom-Lang, 1955; Woodward et al., 1982; Englander & Kallenbach, 1984). Although tritium exchange in intact proteins was used to detect structural and dynamic changes in small and large proteins, information about structural changes within specific regions of a protein generally was unavailable. The protein fragmentation method, as originally implemented using tritium, has been used to obtain isotopic exchange rates in small parts of a few larger proteins (Mallikarachchi et al., 1989; Englander et al., 1985; Englander et al., 1992). The present study is the first in which peptide amide hydrogen exchange rates in short segments of most of the backbone of a large protein have been determined. Rabbit muscle aldolase is representative of large proteins because, with a molecular weight of 157 000, tetrameric aldolase is approximately 10-fold larger than the largest proteins routinely studied by high-resolution NMR. Each subunit of the aldolase tetramer has a parallel β-barrel motif, which contains 12 α-helices and 8 β-strands. Results of this study provide an opportunity to determine whether our present understanding of hydrogen exchange in small proteins can be extended to much larger, structurally more complex proteins.

Rate constants for peptide amide hydrogen exchange in short segments (mean length of five residues) derived from 85% of the backbone of rabbit muscle aldolase are given in Table 1. Although the range of isotope exchange rate constants determined in this study spanned nearly 5 orders of magnitude, it is apparent that some amide hydrogens have rate constants greater than 100 h^{-1}, while others have rate constants less than 0.001 h^{-1}. Even within short segments, amide hydrogens undergo isotopic exchange at very different rates. For example, within the short segment comprising residues 59−62, one hydrogen exchanges with a rate constant of 9 h^{-1} and three exchange with a rate constant of 0.006 h^{-1}. This wide variation of rate constants for amide hydrogens located in the same proximity along the backbone is typical of hydrogen exchange in small proteins (Radford et al., 1992; Kim et al., 1993; Bai et al., 1993; Andrec et al., 1995) and suggests that the mechanism for hydrogen exchange for these conditions primarily involves localized dynamics (Radford et al., 1992).

Correlation with Intramolecular Hydrogen Bonding. Results from numerous NMR studies clearly demonstrate that intramolecular hydrogen bonding is a major factor responsible for decreased amide hydrogen exchange rates in small proteins (Pedersen et al., 1991; Constantine et al., 1993). For example, amide hydrogens located in α-helices or β-sheets usually exchange at rates that are several orders of magnitude slower than those of amide hydrogens located in loop regions. To demonstrate a possible correlation between amide hydrogen exchange rates and intramolecular hydrogen bonding, the number of peptide amide hydrogens participating in hydrogen bonds was calculated for each segment of aldolase used in this study. Atomic coordinates for human muscle aldolase (Gamblin et al., 1990; Berstein et al., 1977), which differs in amino acid sequence from rabbit muscle aldolase in only five residues (residues 2−4, 241, and 265),

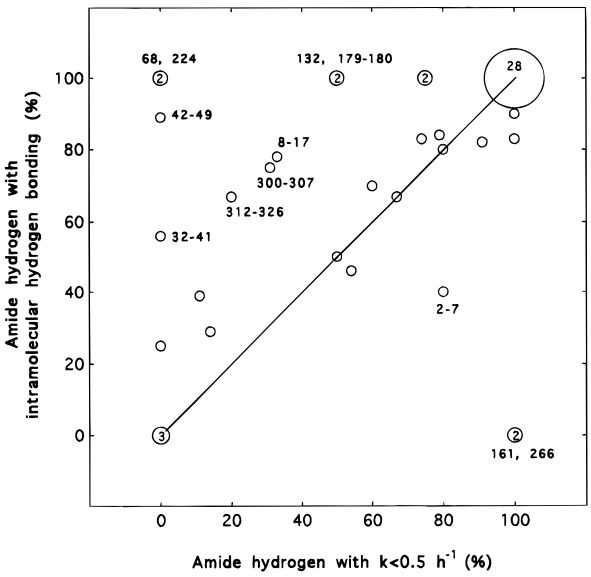

FIGURE 7: Plot of the percentage of peptide amide hydrogens involved in intramolecular hydrogen bonding for each segment versus the percentage of amide hydrogens within these segments that have exchange rate constants of less than 0.5 h^{-1} (data taken from Table 1 of the supporting information). The size of and the number within the circles indicate the number of peptides represented by each circle.

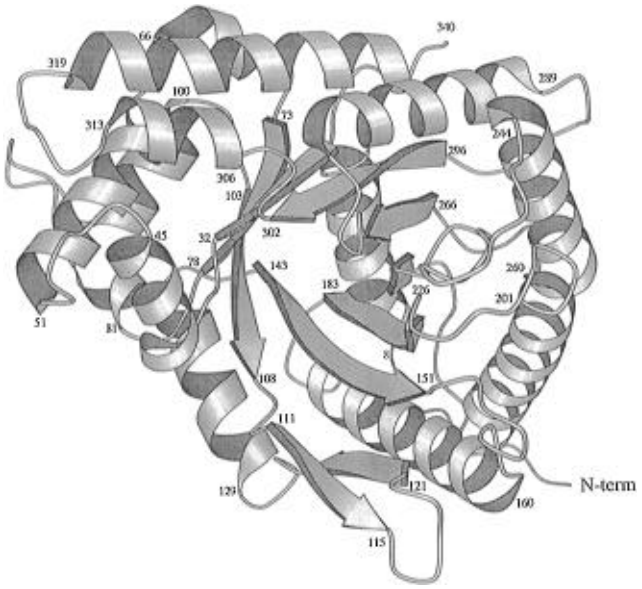

FIGURE 8: Structure of the human aldolase monomer, drawn using *Molscript* (Kraulis, 1991), to indicate the locations of elements of secondary structure (Gamblin et al., 1990; Berstein et al., 1977).

were used for these calculations. These results are presented in Table 1 (supporting information) as the percent of hydrogen-bonded amide hydrogens in each segment. The percentage of amide hydrogens with exchange rates less than 0.5 h^{-1} is also presented in Table 1 for each segment. It is evident from these results that the most slowly exchanging amide hydrogens are located in segments in which the amide hydrogens are participating in intramolecular hydrogen bonding.

To more easily visualize the correlation between intramolecular hydrogen bonding and the slowing of the isotopic exchange reaction, the percentage of peptide amide hydrogens participating in intramolecular hydrogen bonds in each of the sensor peptides used in this study was plotted versus the percentage of amide hydrogens with k_{ex} less than 0.5 h^{-1} in Figure 7. The area of each circle, as well as the number within it, indicates the number of peptides represented by that data point. The strong correlation between amide hydrogen exchange and hydrogen bonding is indicated by the fact that 79% of the segments lie within 20% of the diagonal line. Although a better correlation was obtained when a maximum value for k_{ex} of 10 h^{-1} was used, the smaller value of 0.5 h^{-1} was used for this presentation because it is close to the median value of k_{ex}.

Several segments lie above the diagonal line in Figure 7, indicating that amide hydrogen exchange in these segments is faster than expected for amide hydrogens that are involved in intramolecular hydrogen bonding. For example, the X-ray crystallographic structure of aldolase indicates that eight of the nine amide hydrogens in segment 42−49 are hydrogen bonded to other parts of the molecule, but all exchange rapidly (k_{ex} > 7 h^{-1}). Four segments of longer than three residues have anomalously fast isotopic exchange rates (residues 8−17, 32−49, 300−307, and 312−326). All of these segments have some helical or β-sheet structure (Figure 8). Three of the four segments (8−17, 32−49, and 312−326) are located on the surface of the protein, whereas one segment (300−307) is located in the interior. Three segments are in close proximity to each other (32-49, 300−307, and 312−326) and distal to the tetramer center (Figure 9). Segments 32−49 and 300−307 are also near the active site. Residues 8−17 form part of a helix starting at residue 8 (Figure 8), which closes off the amino end of the β-barrel opposite to the active site at the carboxyl end of the β-barrel. Although the factors responsible for fast exchange in these segments are not understood, Radford et al. (1992) have reported that some short α-helices, as well as the ends of some larger α-helices in lysozyme, also have unusually fast hydrogen exchange rates. It should be noted that other helices on the surface do not have unusually fast exchange rates.

Other segments lie below the diagonal line in Figure 7, indicating that amide hydrogen exchange in these segments is slower than expected from the lower fraction of intramolecular hydrogen bonding. The crystallographic structure indicates that the N-terminal segment, including amide linkages 2−7, is an extended structure with only two amide hydrogens participating in intramolecular hydrogen bonding (Figure 8). However, results in Table 1 (supporting information) show that the rate constant for the most rapidly exchanging amide hydrogen in this segment is approximately 10−100-fold less than that for other peptides lacking amide hydrogen bonds. This segment is located in the tetrameric interface (Figure 10) where the N-terminal amine of residue 1 of one subunit forms a hydrogen bond with the main chain of residue 158 from a second subunit. The N-terminal residues 1−7 are tucked into the central core of the tetramer and in close proximity to residue 161, another residue with unexpectedly slow exchange. Residue 266, another residue that is not hydrogen bonded but slow to exchange, lies at the larger of the two contact regions between subunits (Gamblin et al., 1990). Thus, the strong interaction at this interface appears to slow hydrogen exchange and access by solvent molecules to an extent similar to the surrounding helices and strands that make up this interface.

From this analysis of intramolecular hydrogen bonding and amide hydrogen exchange rates, it is evident that the two

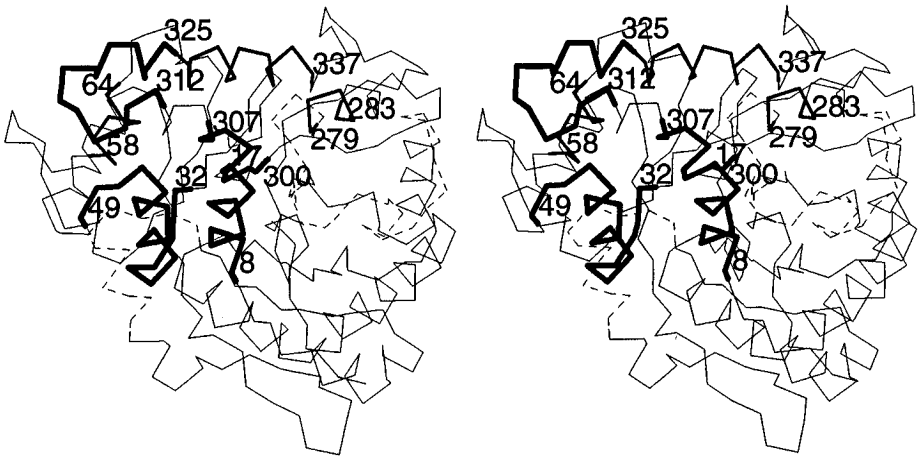

FIGURE 9: Stereoview of human aldolase monomer, oriented as in Figure 8, indicating (1) regions where hydrogen exchange is faster than expected from intramolecular hydrogen bonding (thick line); (2) regions where bimodal isotope patterns were found (medium line); and (3) regions for which no peptides were detected in this study (dashed line).

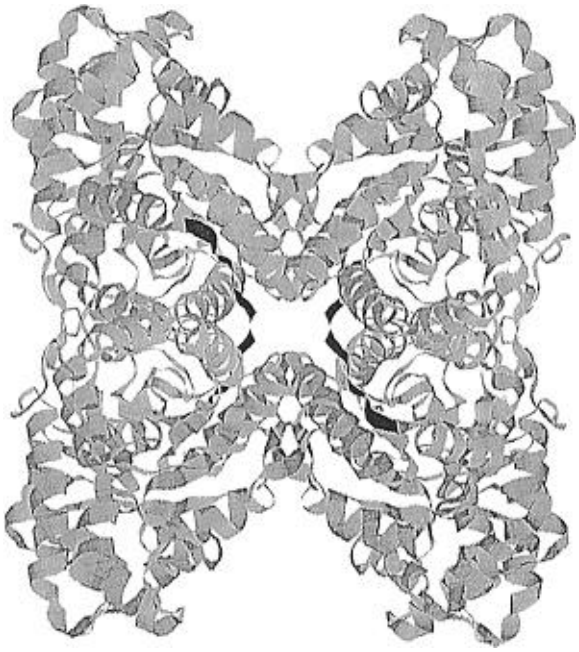

FIGURE 10: Structure of human aldolase tetramer, drawn with *Molmass*, illustrating that the segment including residues 2−7 (darkened region) is located on the subunit binding surface.

are highly correlated, as in much smaller proteins (Englander & Kallenbach, 1984; Radford et al., 1992). In addition, large hydrophobic contact surfaces, such as those through which the aldolase monomers are joined, may shield some amide hydrogens from the solvent, thereby decreasing the rates of isotopic exchange by factors as large as 10^6.

Prediction of Secondary Structure. Correlation of hydrogen exchange data with intramolecular hydrogen bonding, as presented in Figure 7, is possible only if a high-resolution three-dimensional structure is available. However, given the correlation between intramolecular hydrogen bonding and the slowing of hydrogen exchange rates, it may be possible to use amide hydrogen exchange rates to predict the approximate locations of secondary structural elements in large proteins. Similarly, NMR structural determination methods utilize hydrogen exchange rates in combination with NOE and *J* coupling information to locate secondary structure, although exceptions to the most slowly exchanging amides being in secondary structure have been noted (Pedersen et al., 1991). To investigate the potential of amide hydrogen exchange as a tool for locating elements of secondary structure in large proteins, we have considered the likelihood that an amide hydrogen exchanges faster than specified arbitrary limits, chosen here to be 0.01, 0.1, 1.0, and 10 h^{-1}. From the distribution of rate constants and the number of amide positions in a peptide, it follows that each amide hydrogen within a specific segment has a probability that its rate constant will be greater than a specified value. This concept may be illustrated for the segment 300−307, which has eight amide hydrogens. Isotopic exchange results presented in Table 1 (supporting information) for this segment indicate that four hydrogens have exchange rate constants of 53 h^{-1}, three have rate constants of 0.5 h^{-1}, and one has a rate constant of 0.003 h^{-1}. In accordance with these results, the probability that the exchange rate constants for peptide amide hydrogens within the 300−307 segment have a value greater than 10 h^{-1} is 0.5 (4/8). Likewise, the probabilities that these rate constants will be greater than 1, 0.1, or 0.01 h^{-1} are 0.5, 0.88, and 0.88, respectively.

The probabilities that individual amide hydrogens will have exchange rate constants greater than 0.01, 0.1, 1.0, and 10 h^{-1} are given in Figure 11 as a function of their positions along the aldolase backbone. The probability within each panel ranges from 0 to 1, where low probability indicates that the rate constant for isotopic exchange of a particular amide hydrogen is unlikely to be greater than the rate constant designated for that panel. The bottom panel indicates the likelihood that a particular peptide amide hydrogen exchanges very rapidly (k > 10 h^{-1}), while the top panel indicates the likelihood that this hydrogen exchanges very slowly (k > 0.01 h^{-1}). This graphical presentation facilitates the visualization of isotopic exchange rates along the entire backbone of the protein. This feature may be particularly useful for analyses of proteins when their three-dimensional structures are not available.

To illustrate the correlation between slow hydrogen exchange and secondary structure, α-helices and β-sheets are indicated by ovals and rectangles along the x-axis of Figure 11. One can see that the amide hydrogens in α-helices or β-sheets generally have slow exchange rates. For example, among several slowest exchanging segments, amide hydrogens on residues 75−78, 145−151, and 263−269 are in β-sheets, and amide hydrogens on residues 162−174, 203−218, 252−258, and 328−336 are in α-helices.

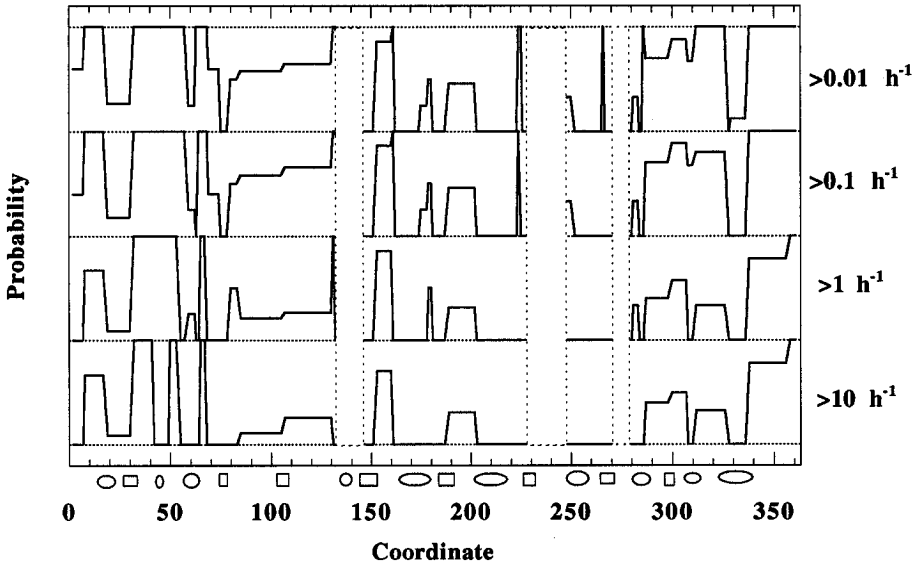

FIGURE 11: Probabilities that peptide amide hydrogens have exchange rate constants greater than 0.01, 0.1, 1.0, and 10 h^{-1}. α-Helices and β-sheets are shown by ovals and rectangles, respectively, along the abscissa.

Although these predictions are only semiquantitative, they do indicate regions in which α-helices and β-sheets are likely to be found without the aid of a three-dimensional structure.

Interpretation of Isotope Patterns. Although the average deuterium level in a segment of protein can be determined by NMR, the distribution of deuterium among the protein molecules in a sample cannot be determined readily by NMR. However, mass spectrometry is unique in that the distribution of deuterium among all of the protein molecules in a sample can be determined from the isotope pattern observed in the mass spectrum of the protein (Miranker et al., 1993). Similarly, the intermolecular distribution of deuterium in specific segments of a protein can be determined from the isotope patterns in the mass spectra of peptides derived from the protein. The distribution of deuterium among the peptide molecules may be an important source of information regarding either the homogeneity of a sample or the mechanism through which isotopic exchange has occurred.

Currently accepted mechanisms for hydrogen exchange involve a two-step process in which a structural change occurs in the native state of a protein to facilitate isotopic exchange (Woodward et al., 1982; Englander & Kallenbach, 1984). The structural change may involve a region as small as a few square angstroms, facilitating the exchange of one amide hydrogen, it may involve a short segment of the protein, facilitating the exchange of several amide hydrogens within this segment, or it may involve global unfolding of the entire protein, facilitating the exchange of all amide hydrogens in the protein. Furthermore, hydrogen exchange may occur through two or more of these mechanisms within the same molecule. The two steps required for hydrogen exchange are illustrated in eq 3. The equilibrium concentra-

$$\mathrm{f(H)} \underset{k_{-1}}{\overset{k_1}{\rightleftharpoons}} \mathrm{u(H)} \xrightarrow{k_2} \mathrm{u(D)} \underset{k_1}{\overset{k_{-1}}{\rightleftharpoons}} \mathrm{f(D)} \qquad (3)$$

tions of the two structural forms are described by an equilibrium constant, K_{unf}, where $K_{unf} = k_1/k_{-1}$. If $k_{-1} >> k_2$, the structural change facilitating hydrogen exchange occurs many times before isotopic exchange occurs, and isotopic exchange is described by EX2 kinetics (Hvidt & Nielsen, 1966; Roder et al., 1985; Bai et al., 1993). If $k_{-1} \ll k_2$, all sites exposed to the deuterated solvent will undergo isotopic exchange in the first opening, and the mechanism is described by EX1 kinetics.

Since exchange via EX2 kinetics leads to a random distribution of deuterium among the peptide units, the isotope pattern observed in the mass spectrum of peptides partially deuterated via a random mechanism will be binomial. The width of the isotope pattern depends on the number of amide linkages and the average deuterium level in a peptide. In contrast, hydrogen exchange via EX1 kinetics leads to a mixture of peptide molecules with regions that either have no deuterium or are fully deuterated. When the unfolding process includes all of the residues in a peptide, the amide hydrogens in this peptide will be either fully protiated or fully deuterated. Since some isotopic exchange occurs during digestion and analysis, the recorded isotope patterns of these peptides are identical with those detected for the same peptides found in the 0% and 100% reference standards. As a result, segments that are deuterated under EX1 conditions have bimodal isotope patterns that can be described by two binomial distributions.

The isotope patterns observed for 53 of the 64 peptides used in this study have the form of a binomial, as illustrated in Figure 2. However, nine peptides derived from segments 58−64, 279−283, and 326−337 have bimodal distributions similar to the one illustrated in Figure 5. Best fits between these isotope patterns and the deuterium distribution model described in the Appendix indicate that the average deuterium level of the peptide units composing the low-mass envelope of each peptide increased with deuterium exchange-in time. This behavior is expected for isotopic exchange proceeding via EX2 kinetics. In contrast, the deuterium level in the high-mass envelope indicated that the protein had been completely deuterated in this segment and did not change with deuterium exchange-in time. This behavior is consistent with hydrogen exchange proceeding via EX1 kinetics. Further analysis of the bimodal isotope patterns for these peptides showed that the portion of the peptide units composing the high-mass envelope (EX1 exchange) increased from 0 to apparent plateau values of 15−20% as the deuterium exchange-in time was increased from 2 min to 44 h. Failure of the high-mass

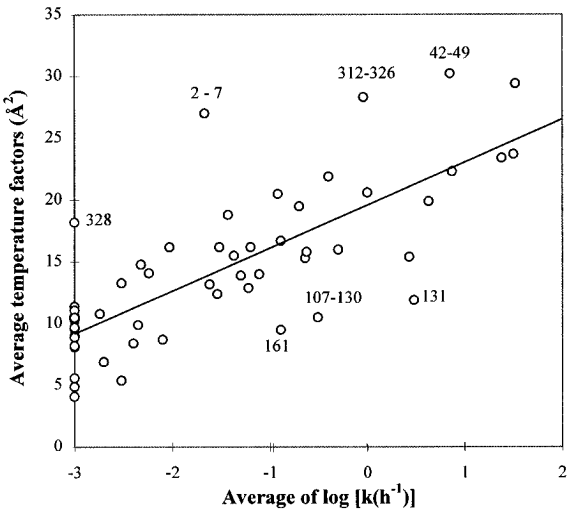

FIGURE 12: Plot of the effective temperature, as calculated from crystallographic *B*-factors, versus the average of the logarithm of the amide hydrogen exchange rate constant for each of the backbone segments of aldolase used in this study.

envelope of peptide units to continue to increase with deuterium exchange-in time is consistent with the existence of two conformers that do not interchange within the time frame of this study. Hydrogen exchange via two competing mechanisms could give a bimodal distribution of isotopes, but the intensity of the high-mass envelope would increase continuously with time. Although a detailed structural difference cannot be ascertained from these data, they do suggest that 20% of the protein is different from the other 80% in that segments 58−64, 279−283, and 326−337 exchange through the EX1 mechanism.

It is of particular interest that all three of these segments occur in the middles of three α-helices (starting at residues 51, 275, and 319) and are in close spatial proximity to each other (Figures 8 and 9). In addition, these segments are near regions with unusually fast amide exchange rates, i.e., those above the diagonal line in Figure 7. Indeed, the segment 300−307, which has unusually fast amide exchange for a segment that is 75% hydrogen bonded, is sandwiched between the bimodal segments 279−287 and 326−337. The other segment showing a bimodal isotope pattern (58−64) packs against segment 312−326, another segment with unusually fast exchange. Although the structural and dynamic processes giving rise to the bimodal isotope distributions are unknown at this time, it is evident from these results that this part of the protein is exhibiting unusual behavior. In a study of the thermal dependence of amide hydrogen exchange rates in aldolase, Zhang and Smith (in preparation) found these three segments to be among the most thermally labile.

The bimodal isotope pattern might be due to misfolding of these α-helices in a small percentage of aldolase molecules used in this study. This explanation is consistent with studies by Chan et al. (1973), who found that the enzymatic activity of aldolase increased by 13% after refolding following denaturation with urea. Alternatively, there may be two active forms of aldolase that do not interconvert on the time scale of these hydrogen exchange experiments. The results of several studies of the enzymatic activity, UV difference spectroscopy, fluorescence, and the reactivity of cysteinyl residues suggest that two reactive states of aldolase coexist in solution (Lehrer & Barker, 1970, 1971; Heyduk & Kochman, 1985; Heyduk et al., 1991).

Correlation with X-ray B-Factors. Under solution conditions of the native protein structure, amide exchange most often proceeds by low-activation-energy processes (Wedin et al., 1982; Thomsen & Poulsen, 1993), which could be reflected by localized positional fluctuations. Thus, it is of interest to consider the relationship between the amide exchange rates and crystallographic *B*-factors. *B*-factors are an indication of the mean-square positional displacements in the protein crystal (Willis & Pryor, 1975), although other parameters also contribute to *B*-factors. The relationship between the amide exchange rates and crystallographic *B*-factors is shown in Figure 12. Values for $\log(k_{ex})$ and *B*-factors were averaged over the segments listed in Table 1 (supporting information), excluding proline residues. To determine the average *B*-factor for a segment, the *B*-factors for the following group of atoms centered on amide nitrogens were included for each amide in the segment:

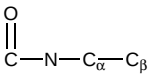

It is clear from Figure 12 that amide hydrogen exchange rates correlate with *B*-factors at the resolution of comparing values averaged over the peptides. The peptide with the greatest deviation (2−7) was also an exceptional case with regard to the correlation between intramolecular hydrogen bonding and rate constants for amide hydrogen exchange. This correlation has not been found in studies of smaller globular proteins (Kossiakoff, 1982; Radford et al., 1992), although common trends, such as an indication of enhanced flexibility in loop regions, has been reported (Constantine et al., 1993). Whether this difference between our results and studies of smaller, monomeric proteins is due to the difference in residue-specific resolution permitted by NMR and crystallography or to intrinsic differences in the dynamic properties of large protein molecules is not yet known.

The time scale of amide exchange is orders of magnitude slower than that for the motions reflected in *B*-factors. Although the structural mechanism for the exchange of buried amide hydrogens from the native state is unknown, exchange must involve numerous dynamic processes and excursions from the average structure that combine to an overall rare event. Together with the wide range of exchange rates, and the extremely large variation within a short peptide, the correlation shown in Figure 12 suggests that amide exchange occurs by events that can be characterized by localized low-amplitude, high-frequency motions that do not require the collective motion of many residues.

Summary. The protein fragmentation/MS method has been used to determine the rates of isotopic exchange in short segments of aldolase with an average length of five residues for 85% of the aldolase backbone. Isotopic exchange rates differing by nearly 5 orders of magnitude were determined. Examination of the three-dimensional structure of aldolase indicates that amide hydrogens with exchange rates of less than 0.5 h^{-1} most often participate in intramolecular hydrogen bonding, while amide hydrogens with exchange rates greater than 0.5 h^{-1} are most often found in loop regions. However, hydrogen exchange in some α-helices is especially fast, suggesting that these particular helices are only weakly formed. Likewise, hydrogen exchange in loops located along

the binding surfaces of the aldolase monomers was much slower than expected, indicating that these regions have limited access to the solvent. The isotope patterns found for most of the sensor peptides were consistent with hydrogen exchange occurring via EX2 kinetics (uncorrelated exchange). However, bimodal isotope patterns were detected for peptides from three regions of aldolase. Modeling of these results indicated that 15−20% of the aldolase used in this study had structural or dynamic variations in these three regions.

These results suggest that the analytical procedures used here may be used to determine amide hydrogen exchange rates in proteins that are much too large to be studied by high-resolution NMR. As long as a protein can be fragmented with an acid protease prior to analysis, there appears to be no limit to the size of protein that can be studied by this approach. Although the spatial resolution of the protein fragmentation/MS method presently is limited to segments containing approximately five residues, Bai et al. (1995) have reported finding subglobal unfolding units in cytochrome *c* containing 15−27 residues. Thus, it might be possible to use this method to detect and characterize such localized unfolding units in suitably destabilized large proteins. With an analytical means of measuring amide hydrogen exchange rates within short segments in place, it is now possible to detect conformational changes, identify contact surfaces, and identify folding intermediates in large proteins, as has been done so elegantly by NMR in studies of small proteins. Furthermore, isotope patterns of peptides derived from partially deuterated proteins may be used to detect structural and dynamical heterogeneity in a sample. This feature may be particularly useful for determining whether over expressed proteins have folded properly.

ACKNOWLEDGMENT

The authors recognize S. W. Englander, M. L. Schneider, and J. Bolin for many helpful discussions and C. Ross for assistance with molecular graphics.

APPENDIX

The purpose of this modeling exercise is to determine a unique distribution of deuteriums among all of the peptides that are derived from a specific protein segment, consistent with an observed bimodal isotope pattern (e.g., Figure 5). It is assumed that the bimodal isotope pattern may be attributed to two groups of peptide molecules, each having a characteristic binomial distribution of deuteriums. The observed bimodal isotope pattern is a combination of these binomial distributions. Assume that specific amide linkages in peptide molecules belonging to group A are either not deuterated or fully deuterated and that specific amide linkages in peptide molecules belonging to group B likewise may be not deuterated or fully deuterated. In addition, assume that some specific amide linkages in group B molecules may be incompletely deuterated (i.e., these positions are deuterated in only some of the molecules in this group). Variables used in the fitting process include the relative number of molecules composing group A, the number of amide linkages in group A peptides that are not deuterated or fully deuterated, and the number of amide linkages in group B peptides that are not deuterated, incompletely deuterated, or fully deuterated. The most probable values of these variables are determined by fitting binomial deuterium distributions calculated from the variables to the observed bimodal isotope pattern.

To calculate a test isotope pattern for group A peptides, assume that a is the relative abundance of group A peptides and n_A and f_A are the number of amide linkages that are not deuterated and fully deuterated in group A peptides, respectively. Since significant isotopic exchange occurs during digestion and HPLC fractionation, n_A and f_A can be determined only through new variables, n and f, which represent deuterium levels detected following digestion and analysis. If these f and n deuteriums are distributed randomly in the f_A and n_A amide positions, the deuterium distribution among the peptides in group A is described by the expansion of the product of two binomials (Brownawell & Fillippo, 1982):

$$[(1-f)+f]^{f_A}[(1-n)+n]^{n_A} \tag{A1}$$

where $f = D_{100\%}/N$ and $n = D_{0\%}/N$. Expansion of the preceding expression gives

$$\begin{aligned} A_{m=i+j} &= \sum_{i=0}^{f_A}\left[\binom{f_A}{i}(1-f)^{f_A-i}f^i\sum_{j=0}^{n_A}\left[\binom{n_A}{j}(1-n)^{n_A-j}n^j\right]\right] \\ &= \sum_{i=0}^{f_A}\sum_{j=0}^{n_A}\left[\binom{f_A}{i}(1-f)^{f_A-i}f^i\binom{n_A}{j}(1-n)^{n_A-j}n^j\right] \end{aligned} \tag{A2}$$

where $\binom{f_A}{i} = i!/[f_A!(f_A - i)!]$. A_m represents the isotope abundance of group A peptides with m deuteriums. The preceding equation can be rewritten as

$$A_{m=i+j} = \sum_{i=0}^{f_A}\sum_{j=0}^{n_A}\left[(1-f)^{f_A}(1-n)^{n_A}\binom{f_A}{i}\left(\frac{f}{1-f}\right)^i\binom{n_A}{j}\left(\frac{n}{1-n}\right)^j\right] \tag{A3}$$

The sum of the terms with all possible combinations of i and j that give the same $i + j = m$ value is the abundance of peptides with m deuteriums.

By following a similar approach, the abundance of peptides composing group B peptides can be calculated from the following expression:

$$\begin{aligned} B_{m=i+j+k} = \sum_{i=0}^{f_B}\sum_{j=0}^{p_B}\sum_{k=0}^{n_B}\Bigg[&(1-f)^{f_B}(1-p)^{p_B}(1-n)^{n_B}\binom{f_B}{i} \\ &\left(\frac{f}{1-f}\right)^i\binom{p_B}{j}\left(\frac{p}{1-p}\right)^j\binom{n_B}{k}\left(\frac{n}{1-n}\right)^k\Bigg] \end{aligned} \tag{A4}$$

Variables f and n are defined as for group A peptides: $f = D_{100\%}/N$ and $n = D_{0\%}/N$. Variable p is the average fractional deuterium level of the partially deuterated peptide linkages, detected after the peptides go through digestion and analysis. The following shows how p is calculated. Let D_p be the number of deuteriums incorporated into p_B partially deuterated peptide linkages before digestion and analysis. Because the deuteration level D, as calculated in eq 1, includes the fully deuterated peptide linkages in group A peptides, the fully deuterated peptide linkages in group B peptides, and D_p partially deuterated peptide linkages group B peptides, i.e., $D = + f_A a + (f_B + D_p)(1 - a)$, then D_p can be calculated by

$$D_p = \frac{D - f_A a}{1 - a} - f_B$$

Within group B peptides, there are p_B peptide linkages that are partially deuterated with deuteration level D_p. Among these p_B peptide linkages in an average peptide molecule, D_p peptide linkages are deuterated, and D_pf deuteriums will be detected following digestion and analysis, assuming that the percent deuterium loss from these peptide linkages is the same as the percent deuterium loss from the group B peptides in the fully deuterated control. It follows that $(p_B - D_p)$ peptide linkages are not deuterated and that $(p_B - D_p)n$ deuteriums will be detected following digestion and analysis, assuming that the deuterium gain at these positions is the same as the deuterium loss from the group B peptides in the nondeuterated control. The measured deuterium level of the partially deuterated hydrogens, p, is then calculated from the following expression:

$$p = \frac{(p_B - D_p)n + D_p f}{p_B}$$

The final deuterium distribution pattern of the peptide, C, is the sum of the binomial distributions calculated for peptide groups A and B:

$$C_m = aA_m + (1 - a)B_m \qquad \text{(A5)}$$

The relative abundance of molecules composing groups A and B, as well as the number of fast and slow exchanging peptide linkages in these groups, can be determined from parameters that give the best fit between the isotope pattern calculated by using this model and the experimental isotope pattern. The validity of this approach was established by combining a fully deuterated protein with a partially deuterated protein in different ratios and analyzing the mixture by the protein fragmentation/MS method. The relative abundance of the fully deuterated protein in the sample was deduced by comparing isotope patterns calculated with this model to the bimodal isotope patterns observed for several peptides (Zhang et al., unpublished results, 1993).

SUPPORTING INFORMATION AVAILABLE

Table 1 containing peptide amide hydrogen exchange rate constants in rabbit muscle aldolase (3 pages). Ordering information is given on any current masthead page.

REFERENCES

Andrec, M., Blake Hill, R., & Prestegard, J. H. (1995) *Protein Sci. 4*, 983−993.

Bai, Y., Milne, J. S., Mayne, L., & Englander, S. W. (1993) *Proteins: Struct., Funct., Genet. 17*, 75−86.

Bai, Y., Sosnick, R. R., Mayne, L., & Englander, S. W. (1995) *Science* (in press).

Baldwin, R. L. (1993) *Curr. Opin. Struct. Biol. 3*, 84−91.

Benjamin, D. C., Williams, D. C., Jr., Smith-Gill, S. J., & Rule, G. S. (1992) *Biochemistry 31*, 9539−9545.

Bentley, G. A., Delepierre, M., Dobson, C. M., Wedin, R. E., Mason, S. A., & Poulsen, F. M. (1983) *J. Mol. Biol. 170*, 243−247.

Bernstein, F. C., Koetzle, T. F., Williams, G. J. B., Meyer, E. F., Jr., Brice, M. D., Rodgers, J. R., Kennard, O., Shimanouchi, T., & Tasumi, M. (1977) *J. Mol. Biol. 112*, 535−542.

Biemann, K. (1990*) Methods Enzymol. 193*, 455−479.

Brandt, P., & Woodward, C. (1987) *Biochemistry 26*, 3156−3162.

Brownawell, M., & Fillippo, J. S., Jr. (1982) *J. Chem. Educ. 59*, 663−665

Caprioli, R. M., & Fan, T. (1986) *Anal. Biochem. 154*, 596−603.

Chan, W., Mort, J. S., Chong, D. K. K., & Macdonald, P. D. M. (1973) *J. Biol. Chem. 248*, 2778−2784.

Constantine, K. L., Friedrichs, M. S., Goldfarb, V., Jeffrey, P. D., Sheriff, S., & Mueller, L. (1993) *Proteins: Struct., Funct., Genet. 15*, 290−311.

de Jong, H. H. J., Goormaghtigh, E., & Ruysschaert, J.-M. (1995) *Biochemistry 34*, 172−179.

Delepierre, M., Dobson, C. M., Karplus, M., Poulsen, F. M., States, D. J., & Wedin, R. E. (1987) *J. Mol. Biol. 197*, 111−130.

Englander, S. W., & Kallenbach, N. R. (1984) *Q. Rev. Biophys. 16*, 521−655.

Englander, S. W., & Mayne, L. (1992) *Annu. Rev. Biophys. Biomol. Struct. 21*, 243−65.

Englander, J. J., Calhoun, D. B., & Englander, S. W. (1979) *Anal. Biochem. 92*, 517−524.

Englander, J. J., Rogero, J. R., & Englander, S. W. (1985) *Anal. Biochem. 147*, 234−244.

Englander, S. W., Englander, J. J., McKinnie, R. E., Jurner, G. J., Westrick, J. A., & Gill, S. J. (1992) *Science 256*, 1684−1687.

Gamblin, S. J., Cooper, B., Millar, J. R., Davies, G. J., Littlechild, J. A., & Watson, H. C. (1990) *FEBS Lett. 262*, 282.

Henry, G. D., & Sykes, B. D. (1990) *Biochemistry 29*, 6303−6313.

Heyduk, T., & Kochman, M. (1985) *Eur. J. Biochem. 151*, 337−343.

Heyduk, T., Michalczyk, R., & Kochman, M. (1991) *J. Biol. Chem. 266*, 15650−15655.

Hughson, F. M., Wright, P. E., & Baldwin, R. L. (1990) *Science 249*, 1544−1548.

Hvidt, A., & Nielsen, S. O. (1966) *Adv. Protein Chem. 21*, 287−385.

Jeng, M. F., Englander, S. W., Elöve, G. A., Wand, J., & Roder, H. (1990) *Biochemistry 29*, 10433−10437.

Johnson, R. S., & Walsh, K. A. (1994) *Protein Sci. 3*, 2144−2418.

Jones, B. E., & Matthews, C. R. (1995) *Protein Sci. 4*, 167−177.

Kaminsky, S. M., & Richards, F. M. (1992) *Protein Sci. 1*, 10−21.

Katta, V., & Chait, B. T. (1991) *Rapid Commun. Mass Spectrom. 5*, 214−217.

Katta, V., & Chait, B. T. (1993) *J. Am. Chem. Soc. 115*, 6317.

Kim, K.-S., Fuchs, J. A., & Woodward, C. K. (1993) *Biochemistry 32*, 9600−9608.

Kossiakoff, A. A. (1982) *Nature 296*, 713−721.

Kraulis, P. J. (1991) *J. Appl. Crystallogr. 24*, 946−950.

Lai, C. Y., Nakai, N., & Chang, D. (1974) *Science 183*, 1204−1205.

Lehrer, G. M., & Barker, R. (1970) *Biochemistry 9*, 1533−1539.

Lehrer, G. M., & Barker, R. (1971) *Biochemistry 10*, 1705−1713.

Linderstom-Lang, K. U. (1955) *Chem. Soc. Spec. Publ.* 2, 1−20.

Liu, Y., & Smith, D. L. (1994) *J. Am. Soc. Mass Spectrom. 5*, 19−28.

Loftus, D., Gbenle, G., Kim, P. S., & Baldwin, R. L. (1986) *Biochemistry 25*, 1428−1436.

Loh, S. N., Prehoda, K. E., Wang, J., & Markley, J. L. (1993) *Biochemistry 32*, 11022−11028.

Louie, T., Tran, T., Englander, J. J., & Englander, S. W. (1988) *J. Mol. Biol. 201*, 755−764.

Mallikarachchi, D., Burz, D. S., & Allewell, N. M. (1989) *Biochemistry 28*, 5386−5391.

Marmorino, J. L., Auld, D. S., Betz, S. F., Doyle, D. F., Young, G. B., & Pielak, G. J. (1993) *Protein Sci. 2*, 1966−1974.

Mayne, L., Paterson, Y., Cerasoli, D., & Englander, S. W. (1992) *Biochemistry 31*, 10678−10685.

McDonald, I. K., & Thornton, J. M. (1994) *J. Mol. Biol. 238*, 777−793.

Miranker, A., Robinson, C. V., Radford, S. E., Aplin, R. T., & Dobson, C. M. (1993) *Science 262*, 896−900.

Molday, R. S., Englander, S. W., & Kallen, R. G. (1972) *Biochemistry 11*, 150−158.

Muga, A., Mantsch, H. H., & Surewicz, W. K. (1991) *Biochemistry 30*, 7219−7224.

Paterson, Y., Englander, S. W., & Roder, H. (1990) *Science 249*, 755−759.

Pedersen, T. G., Sigurskjold, B. W., Andersen, K. V., Kjaer, M., Poulsen, G. M., Dobson, C. M., & Redfield, C. (1991) *J. Mol. Biol. 218*, 413−426.
Radford, S. E., Buck, M., Topping, K. D., Dobson, C. M., & Evans, P. A. (1992*) Proteins: Struct., Funct., Genet. 14*, 237−248.
Roder, H., Wagner, G., & Wüthrich, K. (1985) *Biochemistry 24*, 7396−7407
Rosa, J. J., & Richards, F. M. (1979) *J. Mol. Biol. 133*, 399−416.
Smith, J. B., Sun, Y., Smith, D. L., & Green, B. (1992) *Protein Sci. 1*, 601−608.
Sygusch, J., & Beaudry, D. (1985) *J. Mol. Biol. 186*, 215−217.
Sygusch, J., Boulet, H., & Beaudry, D. (1985) *J. Biol. Chem. 260*, 15286−15290.
Sygusch, J., Beaudry, D., & Allaire, M. (1987) *Proc. Natl. Acad. Sci. U.S.A. 84*, 7846−7850.
Tüchsen, E., & Woodward, C. (1987) *Biochemistry 26*, 8073−8078.
Thomsen, N. K., & Poulsen, F. M. (1993) *J. Mol. Biol 234*, 234−241.
Wagner, G., & Wüthrich, K. (1982) *J. Mol. Biol. 160*, 343−361.
Wagner, D. S., & Anderegg, R. J. (1994) *Anal. Chem. 66*, 706−711.
Wedin, R. E., Delepierre, M., Dobson, C. M., & Poulsen, F. M. (1982) *Biochemistry 21*, 1098−11103.
Willis, B. T. M., & Pryor, A. W. (1975) *Thermal Vibrations in Crystallography*, Cambridge University Press, Cambridge, U.K.
Woodward, C., Simon, I., & Tuchsen, E. (1982) *Mol. Cell. Biochem. 48*, 135−60.
Zhou, Z., & Smith, D. L. (1990) *J. Protein Chem. 9*, 523−532.
Zhang, Z., & Smith, D. L. (1993) *Protein Sci. 2*, 522−531.

BI952227Q